Electronic Supplementary Material (ESI) for Polymer Chemistry.

Anisotropic Polymer Nanoparticles with Solvent and Temperature Dependent Shape and Size from Triblock Copolymers

Elena Bobbi,[1] Bassem Sabagh,[2] Sally-Ann Cryan, [3,4,5] James A. Wilson,[1,5] Andreas Heise[1,5]*

[1]Department of Pharmaceutical and Medicinal Chemistry, Royal College of Surgeons in Ireland (RCSI), 123 St. Stephens Green, Dublin 2, Ireland. [2]Postnova Analytics UK Ltd, Malvern Hills Science Park, Malvern, UK. [3]Trinity Centre for Bioengineering, Trinity College Dublin (TCD), Dublin, Ireland. [4]Drug Delivery & Advanced Materials Team, School of Pharmacy & Tissue Engineering Research Group, Department of Anatomy, Royal College of Surgeons in Ireland (RCSI), 123 St. Stephens Green, Dublin 2, Ireland. [5]Centre for Research in Medical Devices (CURAM), RCSI, Dublin and National University of Ireland, Galway, Ireland.

Table of Contents

1. NMR Spectra 2
2. GPC 7
3. FTIR spectra 10
4. CD spectra 10
   4.1 CD spectra of particles from THF procedure 10
   4.2 CD spectra of particles from HFIP procedure 11
5. AF4 experiments 12
6. DLS experiments 15
   6.1 DLS from THF solvent exchange procedure 15
   6.2 DLS from HFIP solvent exchange procedure 17

1. **NMR Spectra**

H_1 - Phth-poly(NIPAM)$_{79}$-TTC

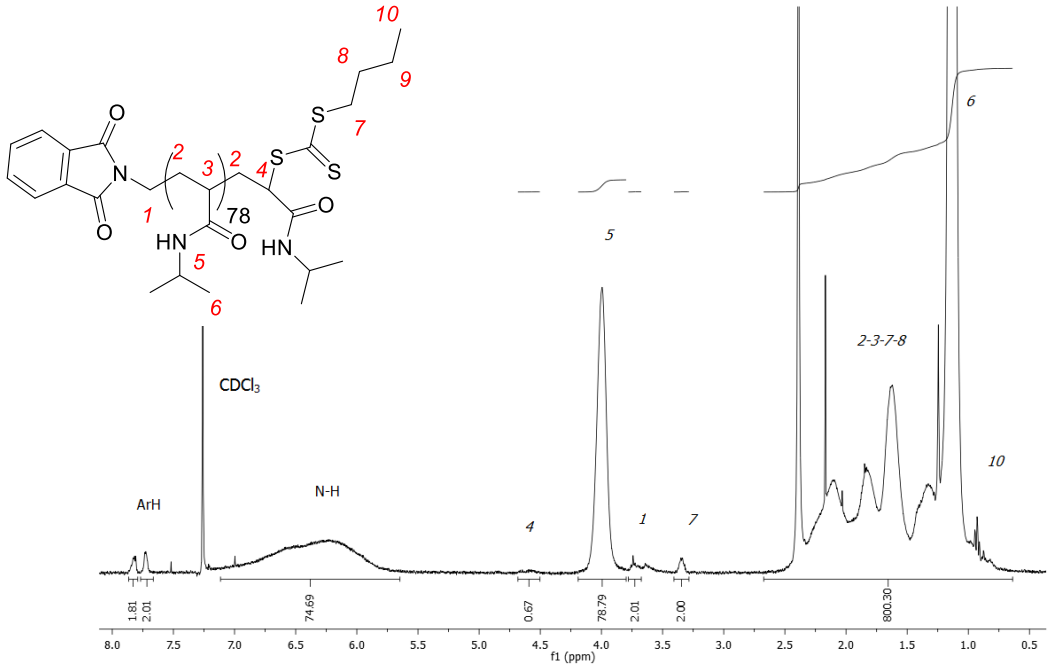

Figure S1: ^{1}H-NMR of H_1 (400 MHz, $CDCl_3$, 303 K) δ = 7.75 (m, 2H, ArH), 7.67 (m, 2H, ArH), 6.22 (br, 79 H, N-H), 4.62 (s, 1 H, -CH(S)C), 4.00 (s, 79 H, -CH(NH)(CH_3)$_2$), 3.73-3.63 (m, 2H, -CH_2-Phth), 3.34 (br, 2H, -$CH_2S(CS_2)$), 2.5-1 (br, acrylic backbone), 1.07 (s, (CH_3)$_2$-CHN-), 0.93 (m, -CH_3) ppm.

D_1 - Phth-poly[(NIPAM)$_{79}$-*b*-(PEGA)$_{66}$]-TTC

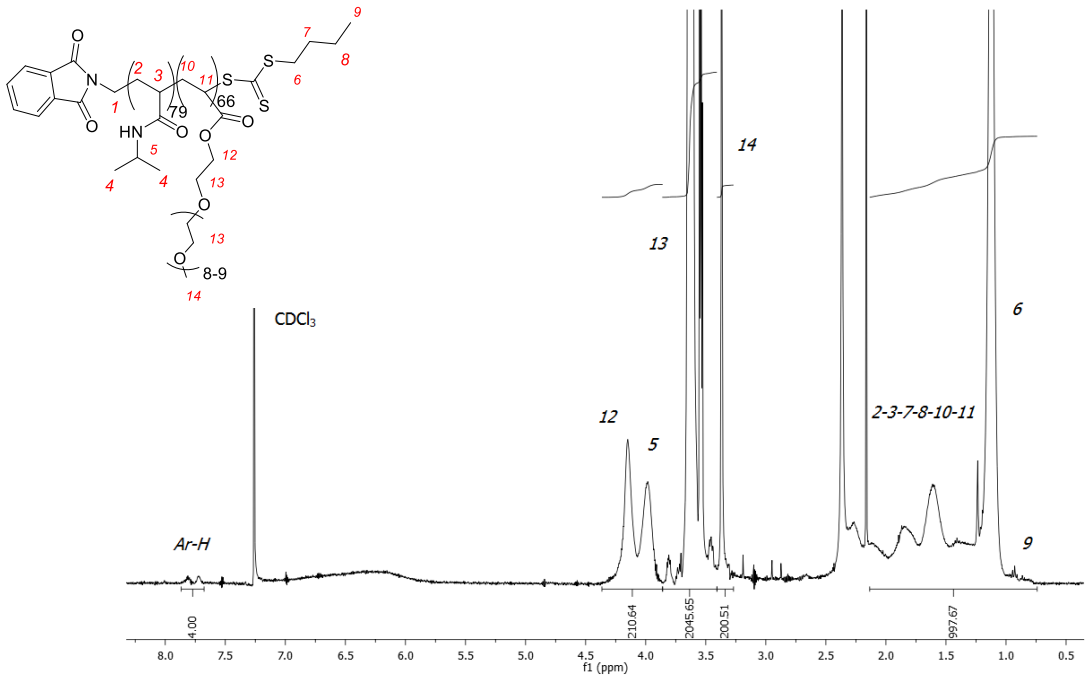

Figure S2: ^{1}H-NMR of D_1 (400 MHz, $CDCl_3$, 303 K) δ = 7.82 (m, ArH), 7.73 (m, ArH), 4.16 (s, -CH_2OC(O)), 4.00 (s, -CH(NH)(CH_3)$_2$), 3.65 (m, -OCH_2CH_2O-), 3.38 (s, -OCH_3), 2.2-1.2 (br, alkyl chain), 1.13 (s, (CH_3)$_2$CHN-), 0.93 (m,-CH_3) ppm.

D_1 - H_2N-poly[(NIPAM)$_{79}$-*b*-(PEGA)$_{66}$]-H

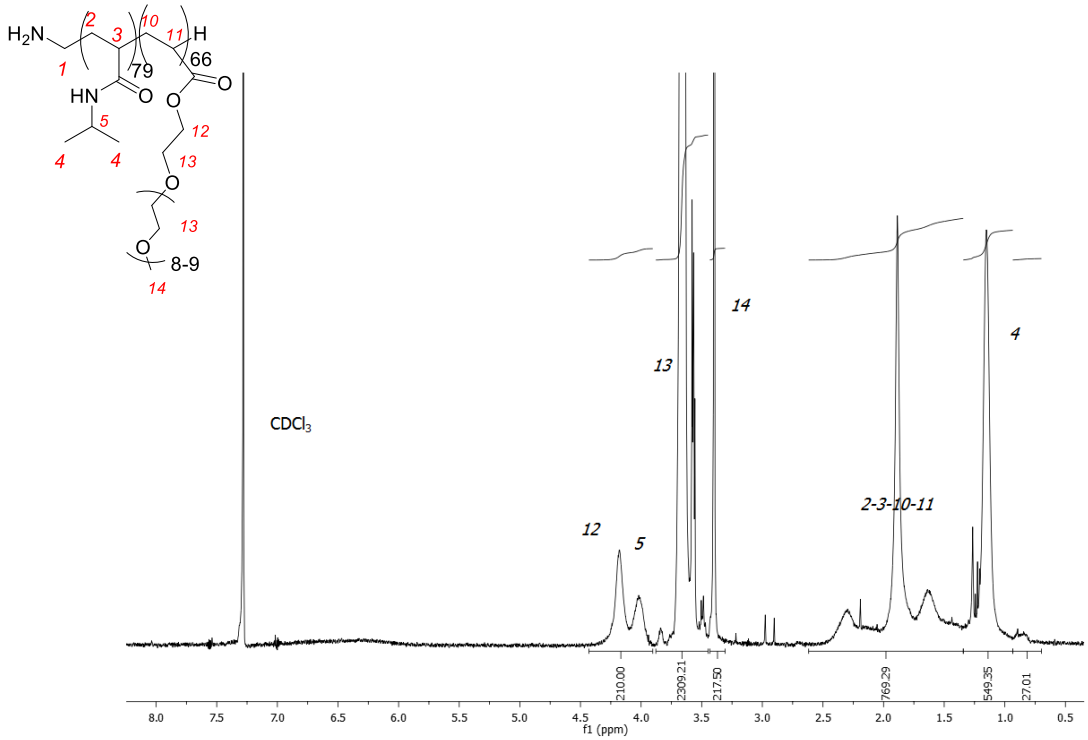

Figure S3: ^{1}H-NMR of D_1 after end cleavages (400 MHz, $CDCl_3$, 303 K) δ = 4.16 (s, -$CH_2OC(O)$), 4.00 (s, -$CH(NH)(CH_3)_2$), 3.65 (m, -OCH_2CH_2O-), 3.38 (s, -OCH_3), 2.2-1.2 (br, alkyl chain), 1.13 (s, $(CH_3)_2CHN$-) ppm.

D_2 - Phth-poly[(NIPAM)$_{79}$-*b*-(PEGA)$_9$]-TTC

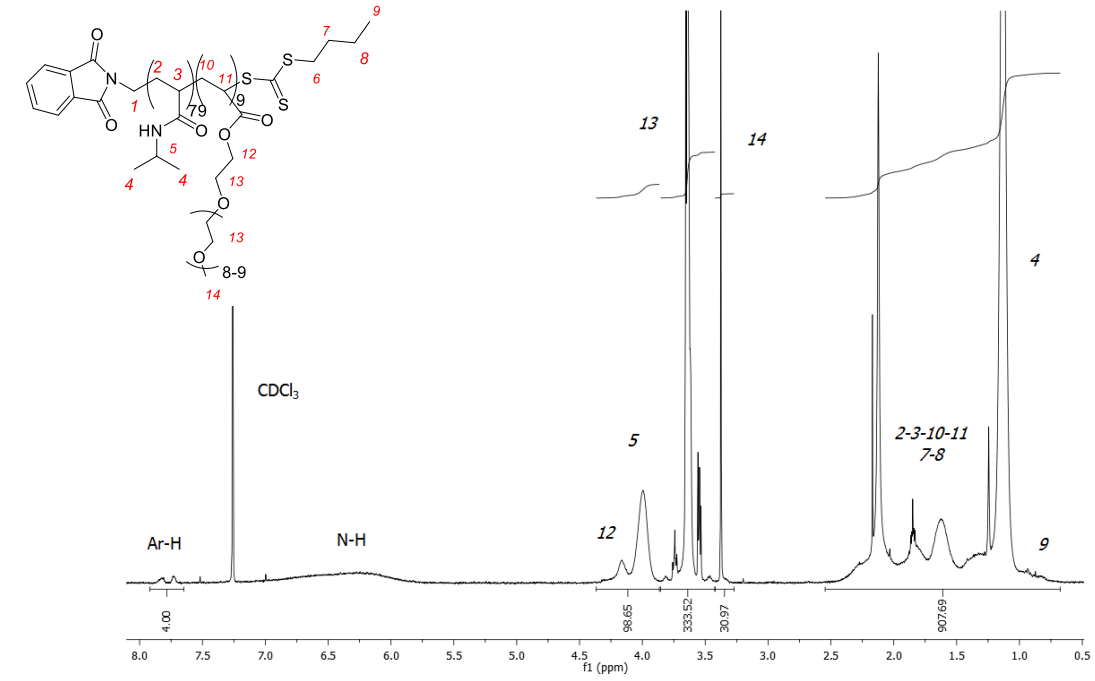

Figure S4: ^{1}H-NMR of D_2 (400 MHz, $CDCl_3$, 303 K) δ = 7.82 (m, ArH), 7.73 (m, ArH), 4.16 (s, -$CH_2OC(O)$), 4.00 (s, -$CH(NH)(CH_3)_2$), 3.65 (m, -OCH_2CH_2O-), 3.38 (s, -OCH_3), 2.2-1.2 (br, alkyl chain), 1.13 (s, $(CH_3)_2CHN$-), 0.93 (m,-CH_3) ppm.

D_2 - H_2N-poly[(NIPAM)$_{79}$-*b*-(PEGA)$_9$]-H

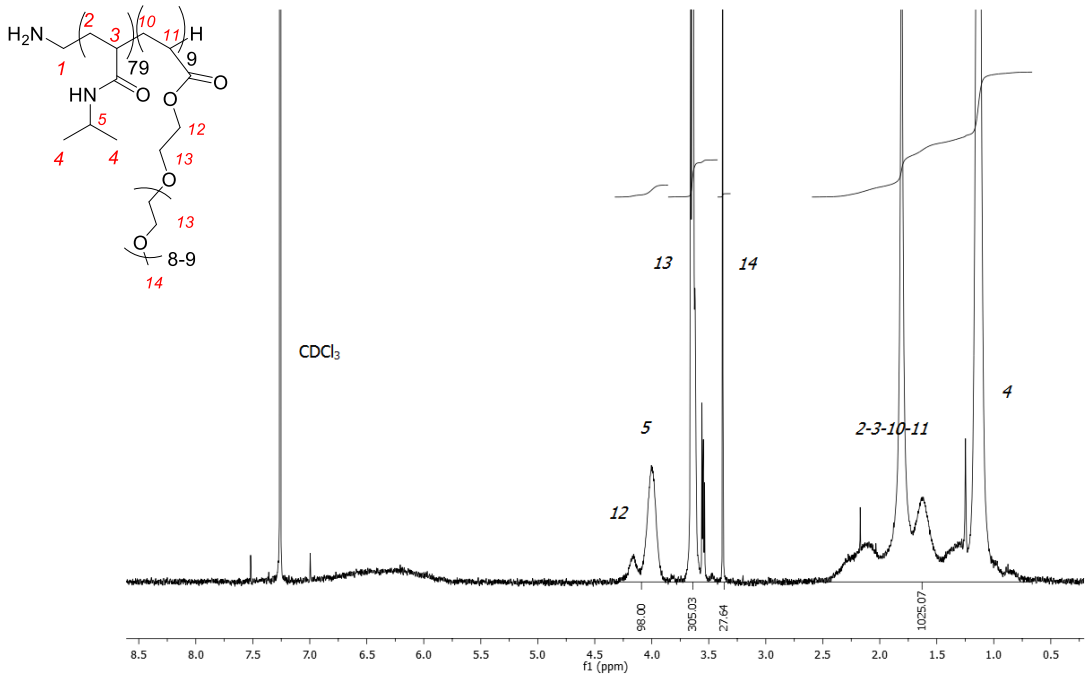

Figure S5: ^{1}H-NMR of D_2 after end cleavages (400 MHz, $CDCl_3$, 303 K) δ = 4.16 (s, -$CH_2OC(O)$), 4.00 (s, -$CH(NH)(CH_3)_2$), 3.65 (m, -OCH_2CH_2O-), 3.38 (s, -OCH_3), 2.2-1.2 (br, alkyl chain), 1.13 (s, $(CH_3)_2CHN$-) ppm.

$T_{1.1}$ - poly[(BLG)$_{60}$-*b*-(NIPAM)$_{79}$-*b*-(PEGA)$_{66}$]

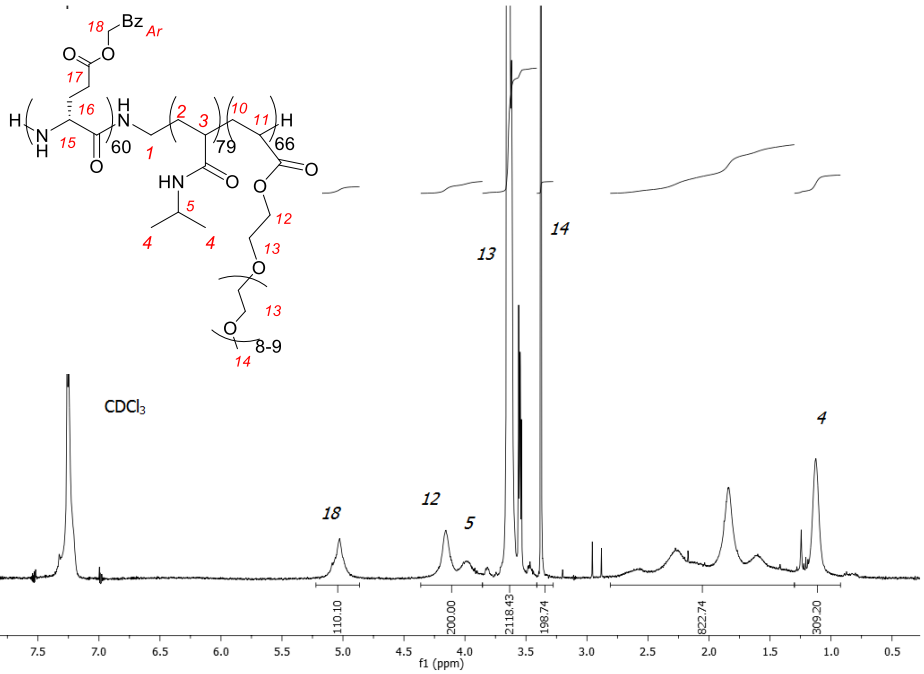

Figure S6: ^{1}H-NMR of $T_{1.1}$ (400 MHz, $CDCl_3$, 303 K) δ = 7.25 (m, Bz), 5.03 (br, -CH_2Ph), 4.17 (s, -$CH_2OC(O)$ PEGA unit), 4.00 (s, -$CH(NH)(CH_3)_2$), 3.65 (m, -OCH_2CH_2O-), 3.38 (s, -OCH_3), 2.2-1.2 (br, alkyl chain), 1.13 (s, $(CH_3)_2CHN$) ppm.

$T_{1.2}$ - poly[$(BLG)_{30}$-*b*-$(NIPAM)_{79}$-*b*-$(PEGA)_{66}$]

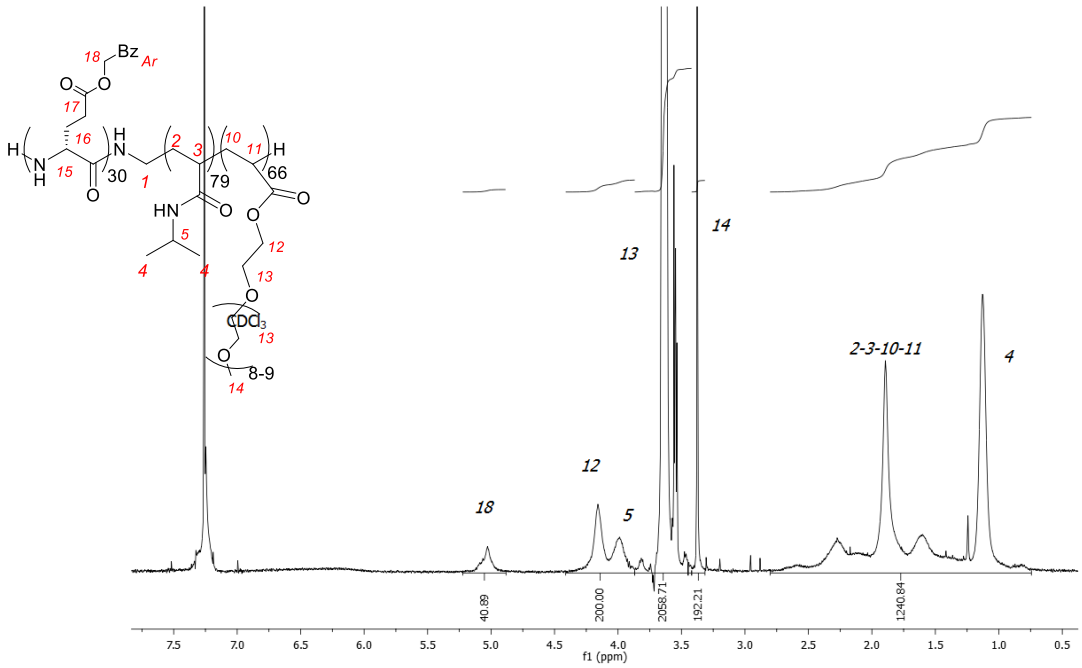

Figure S7: ^{1}H-NMR of T $_{1.2}$ (400 MHz, $CDCl_3$, 303 K) δ = 7.25 (m, Bz), 5.03 (br, -CH_2Ph), 4.17 (s, -$CH_2OC(O)$ PEGA unit), 4.00 (s, -$CH(NH)(CH_3)_2$), 3.65 (m, -OCH_2CH_2O-), 3.38 (s, -OCH_3), 2.2-1.2 (br, alkyl chain), 1.13 (s, $(CH_3)_2CHN$-) ppm.

$T_{1.3}$ - poly[$(BLG)_{7}$-*b*-$(NIPAM)_{79}$-*b*-$(PEGA)_{66}$]

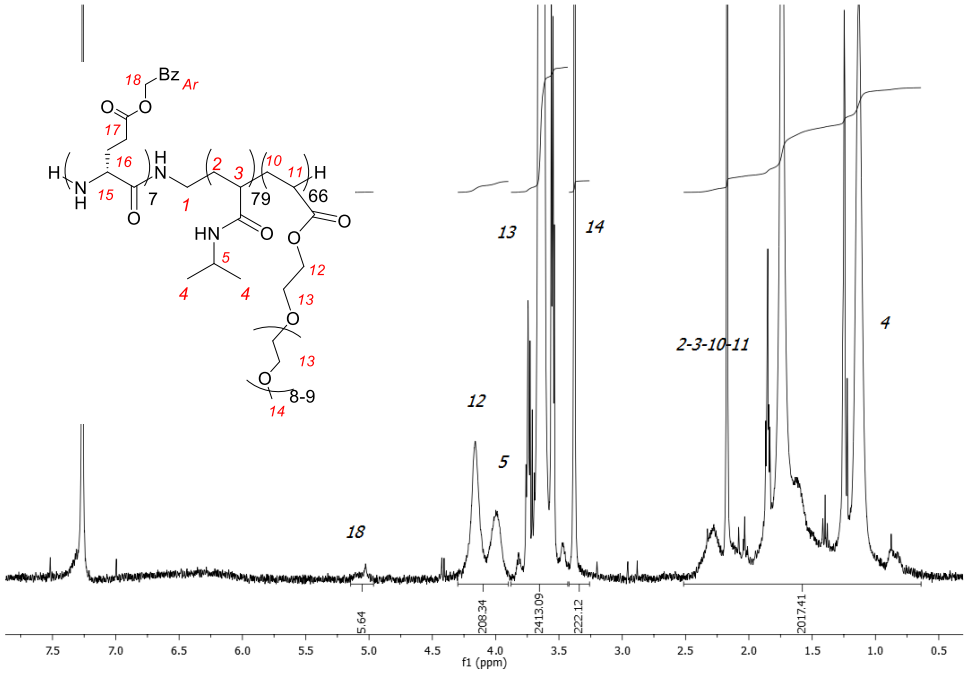

Figure S8: ^{1}H-NMR of T $_{1.3}$ (400 MHz, $CDCl_3$, 303 K) δ = 7.25 (m, Bz), 5.03 (br, -CH_2Ph), 4.17 (s, -$CH_2OC(O)$ PEGA unit), 4.00 (s, -$CH(NH)(CH_3)_2$), 3.65 (m, -OCH_2CH_2O-), 3.38 (s, -OCH_3), 2.2-1.2 (br, alkyl chain), 1.13 (s, $(CH_3)_2CHN$-) ppm.

$T_{2.1}$ - poly[$(BLG)_{60}$-*b*-$(NIPAM)_{79}$-*b*-$(PEGA)_9$]

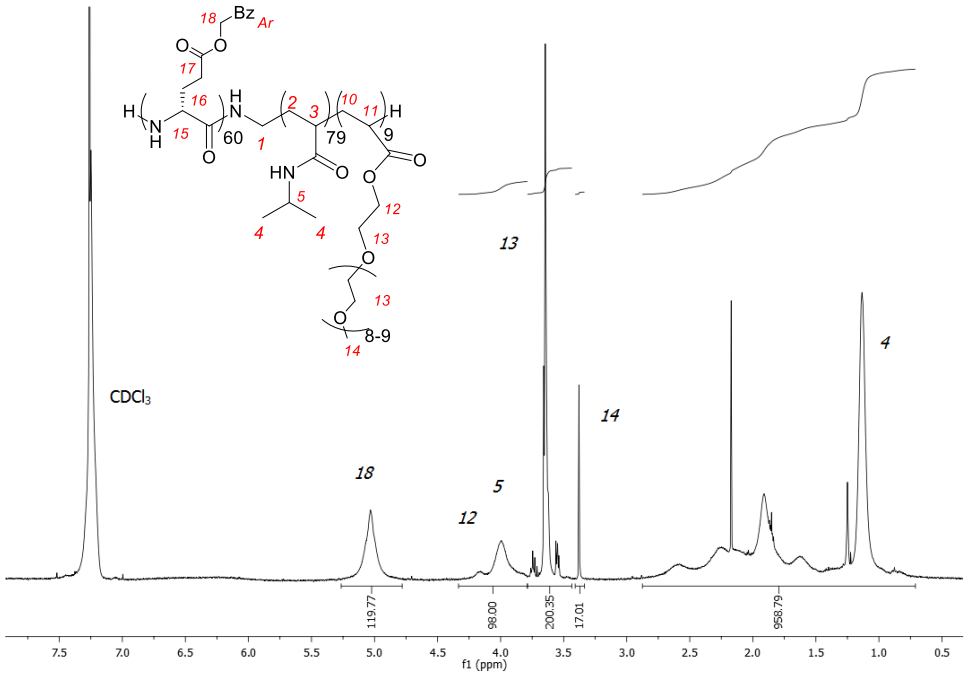

Figure S9: ^{1}H-NMR of $T_{2.1}$ (400 MHz, $CDCl_3$, 303 K) δ = 7.25 (m, Bz), 5.03 (br, -CH_2Ph), 4.17 (s, -$CH_2OC(O)$ PEGA unit), 4.00 (s, -$CH(NH)(CH_3)_2$), 3.65 (m, -OCH_2CH_2O-), 3.38 (s, -OCH_3), 2.2-1.2 (br, alkyl chain), 1.13 (s, $(CH_3)_2CHN$-) ppm.

$T_{2.2}$ - poly[$(BLG)_{30}$-*b*-$(NIPAM)_{79}$-*b*-$(PEGA)_9$]

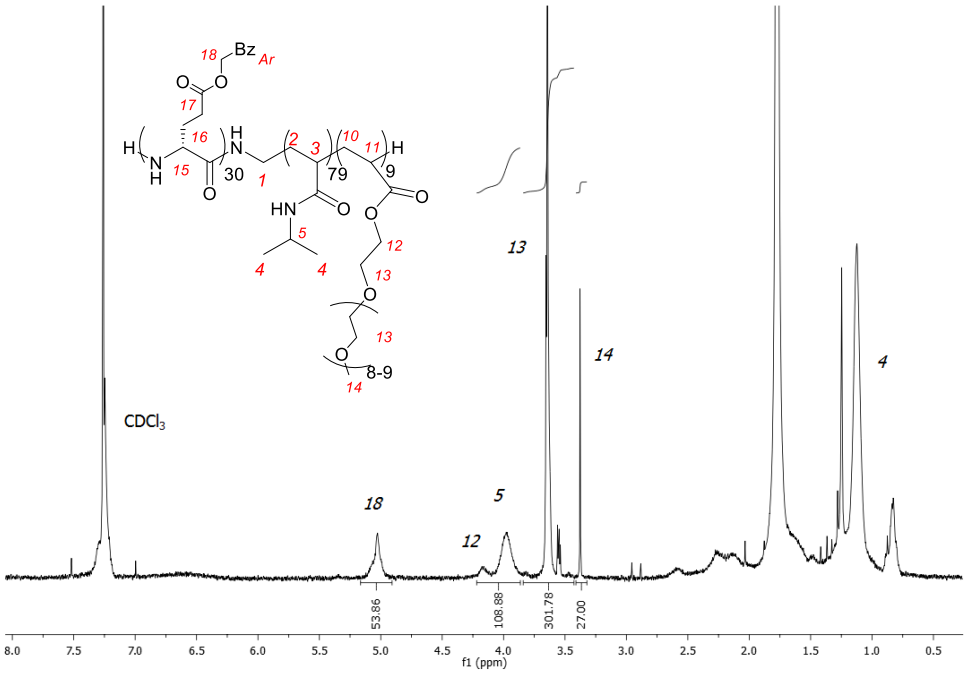

Figure S10: ^{1}H-NMR of $T_{2.2}$ (400 MHz, $CDCl_3$, 303 K) δ = 7.25 (m, Bz), 5.03 (br, -CH_2Ph), 4.17 (s, -$CH_2OC(O)$ PEGA unit), 4.00 (s, -$CH(NH)(CH_3)_2$), 3.65 (m, -OCH_2CH_2O-), 3.38 (s, -OCH_3), 2.2-1.2 (br, alkyl chain), 1.13 (s, $(CH_3)_2CHN$-) ppm.

$T_{2.3}$ - poly[$(BLG)_7$-*b*-$(NIPAM)_{79}$-*b*-$(PEGA)_9$]

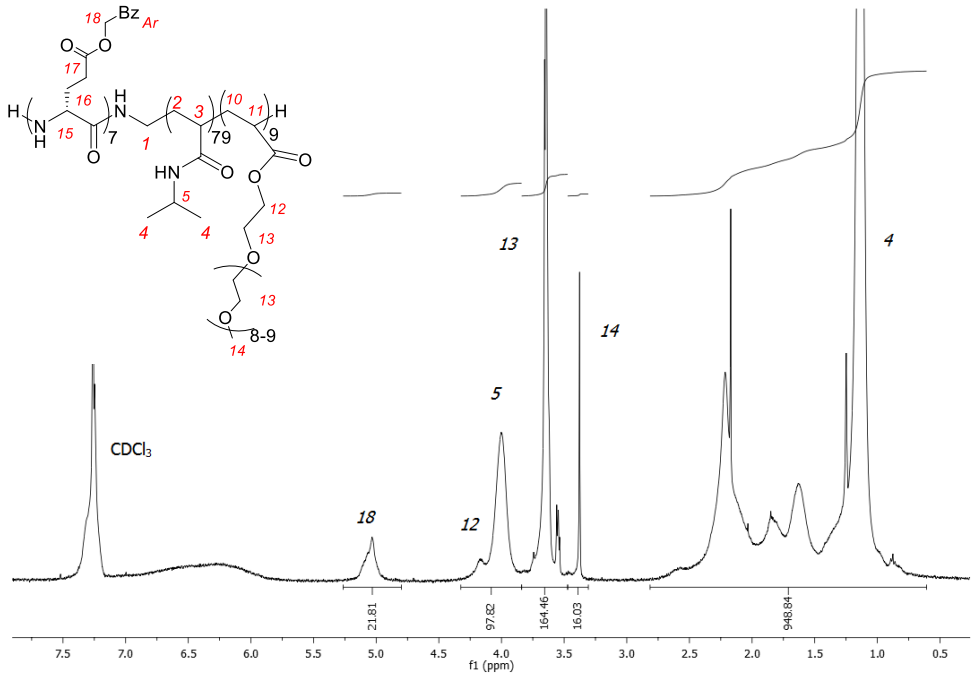

Figure S 11: ^{1}H-NMR of T $_{2.3}$ (400 MHz, $CDCl_3$, 303 K) δ = 7.25 (m, Bz), 5.03 (br, -CH_2Ph), 4.17 (s, -CH_2OC(O) PEGA unit), 4.00 (s, -CH(NH)(CH_3)$_2$), 3.65 (m, -OCH_2CH_2O-), 3.38 (s, -OCH_3), 2.2-1.2 (br, alkyl chain), 1.13 (s, (CH_3)$_2$CHN-) ppm.

2. GPC

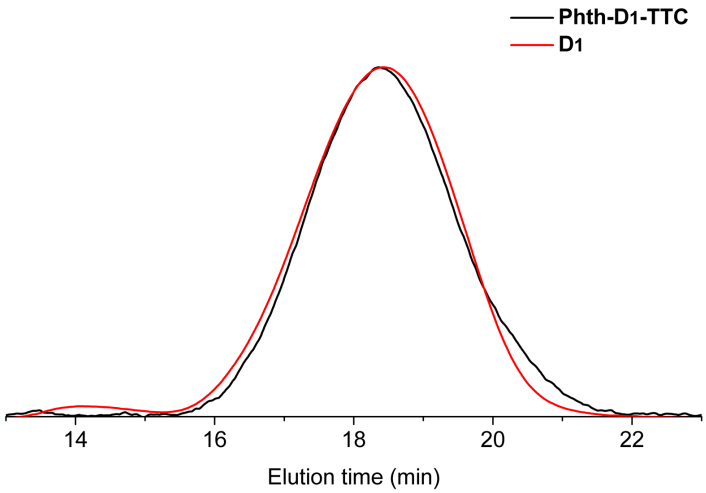

Figure S12: SEC trace of Phth-poly[(NIPAM)$_{79}$-*b*-(PEGA)$_{66}$]-TTC Phth-D$_1$-TTC (black) and poly[(NIPAM)$_{79}$-*b*-(PEGA)$_{66}$] (red). (DMF/LiBr, MALLS detection, 1 mL min^{-1}, molecular mass determined against poly(styrene) standards).

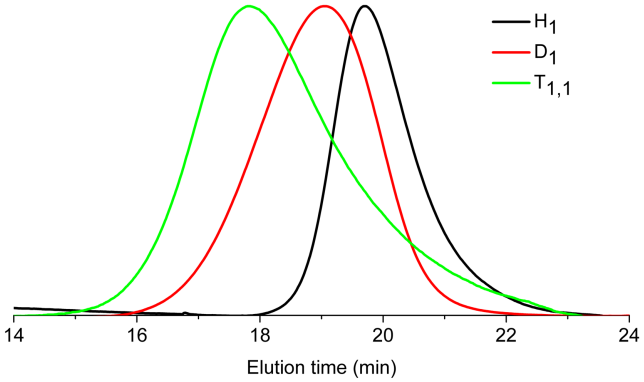

Figure S13: SEC traces (DMF/LiBr, dRI detection, molecular masses determined against poly(styrene) standards) of $T_{1.1}$. $\bar{M}_w$ = 17.3x10^3 g mol^{-1}; $\bar{M}_n$ =15.1x10^3 g mol^{-1} $Đ$ = 1.15.

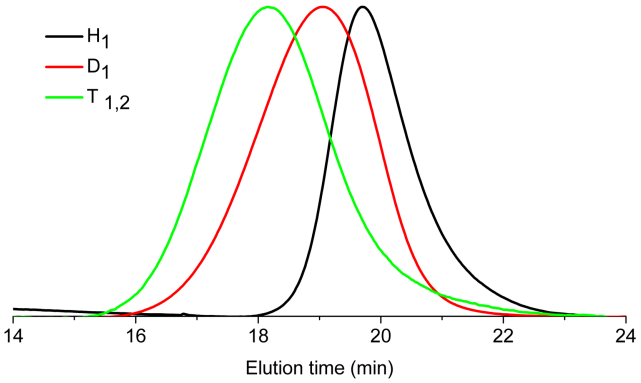

Figure S14: SEC traces (DMF/LiBr, dRI detection, molecular masses determined against poly(styrene) standards) of $T_{1.2}$. $\bar{M}_w$ = 13.7x10^3 g mol^{-1}; $\bar{M}_n$ = 11.3x10^3 g mol^{-1} $Đ$ = 1.21.

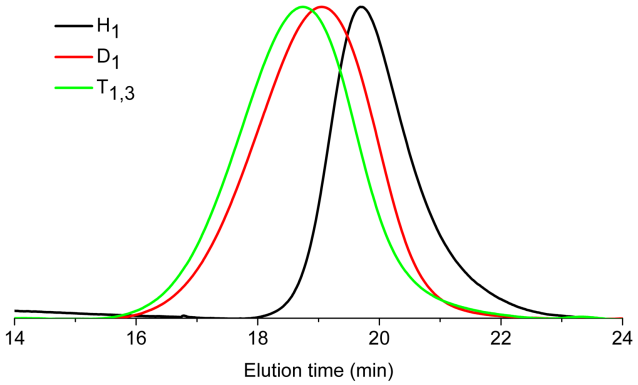

Figure S15: SEC traces (DMF/LiBr, dRI detection, molecular masses determined against poly(styrene) standards) of $T_{1.3}$. $\bar{M}_w$ = 13.9x10^3 g mol^{-1}; $\bar{M}_n$ = 11.1x10^3 g mol^{-1} $Đ$ = 1.26.

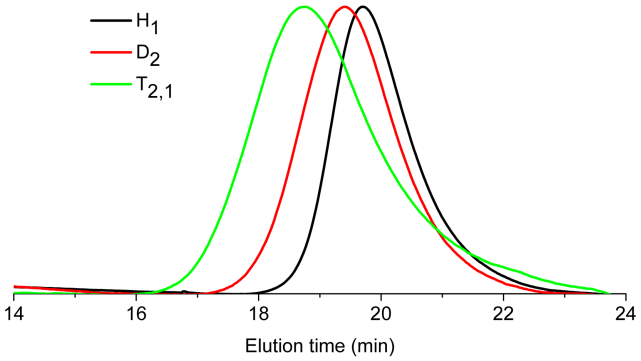

Figure S16: SEC traces (DMF/LiBr, dRI detection, molecular masses determined against poly(styrene) standards) of $T_{2.1}$. $\bar{M}_w$ = 13.3x10^3 g mol^{-1}; $\bar{M}_n$ = 12.3x10^3 g mol^{-1} $Đ$ = 1.08.

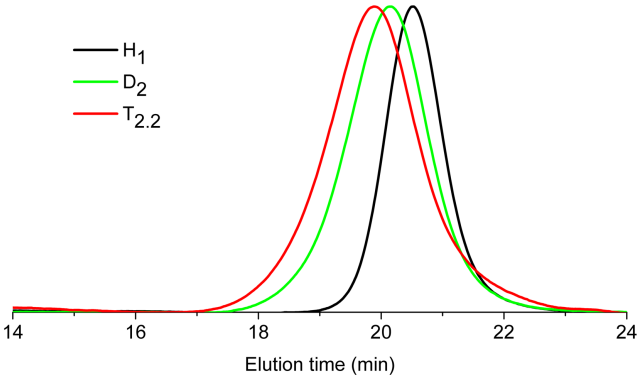

Figure S17: SEC traces (DMF/LiBr, dRI detection, molecular masses determined against poly(styrene) standards) of $T_{2.2}$. $\bar{M}_w$ = 8.60x10^3 g mol^{-1}; $\bar{M}_n$ = 7.84x10^3 g mol^{-1} $Đ$ = 1.10.

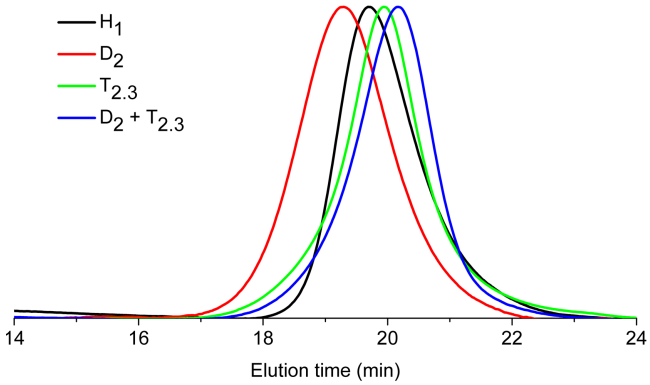

Figure S18: SEC traces (DMF/LiBr, dRI detection, molecular masses determined against poly(styrene) standards) of $T_{2.3}$. $\bar{M}_w$ = 6.32x10^3 g mol^{-1}; $\bar{M}_n$ = 5.76x10^3 g mol^{-1} $Đ$ = 1.10.

3. FTIR spectra

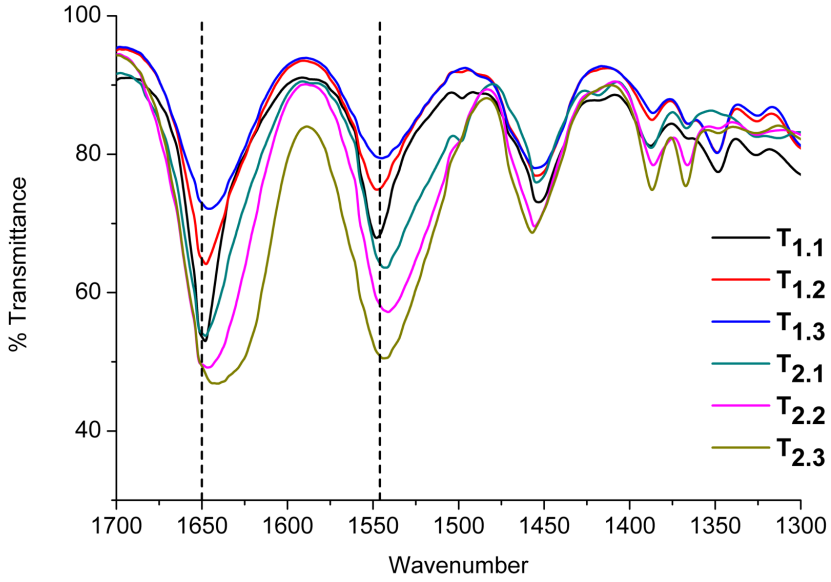

Figure S19: FTIR spectra of solid polymers, dashed lines representing the amide I and II peaks at 1546 and 1650 cm^{-1}.

4. CD spectra

4.1 CD spectra of particles from THF procedure

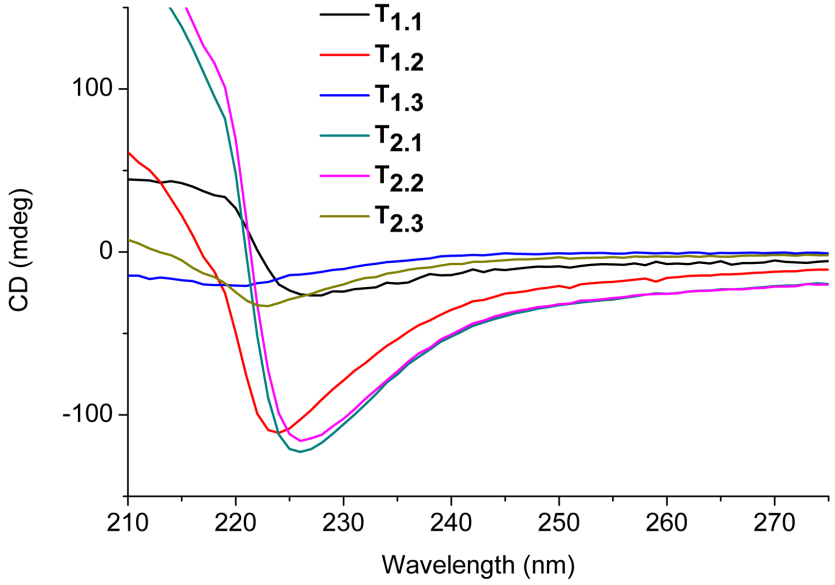

Figure S20: CD spectra of polymers solutions from solvent exchange procedure with THF.

4.2 CD spectra of particles from HFIP procedure

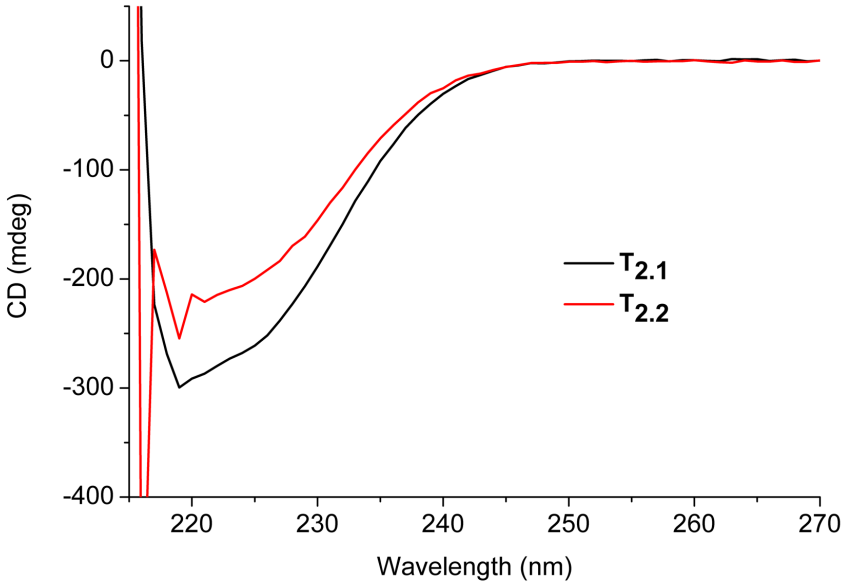

Figure S21: CD spectra of polymers dissolved in HFIP.

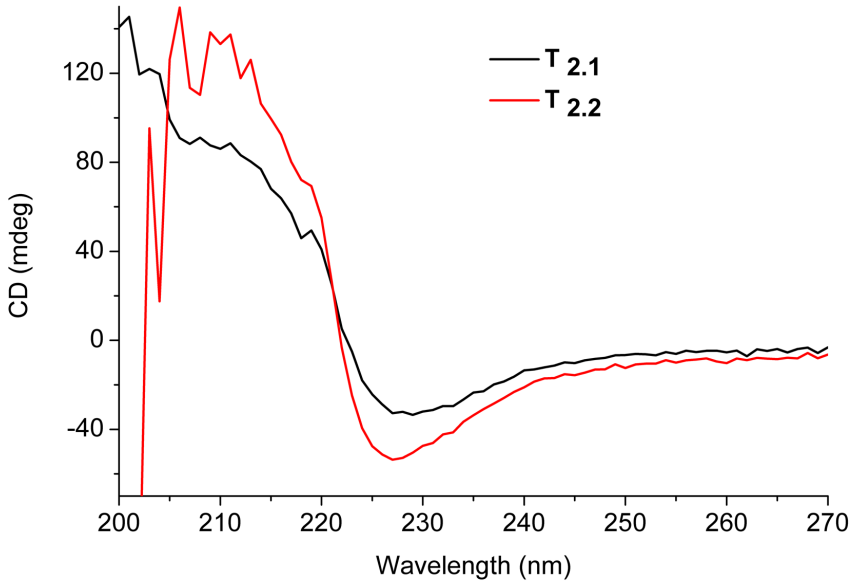

Figure S22: CD spectra of polymers solutions from solvent exchange procedure with HFIP.

5. AF4 experiments

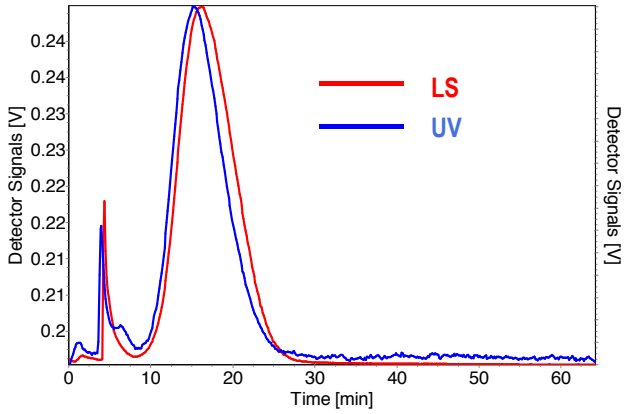

Figure S23: Raw Data Fractogram of AF4 – MALS & UV sample T2.1. The fractogram shows a system peak at ~7 min.

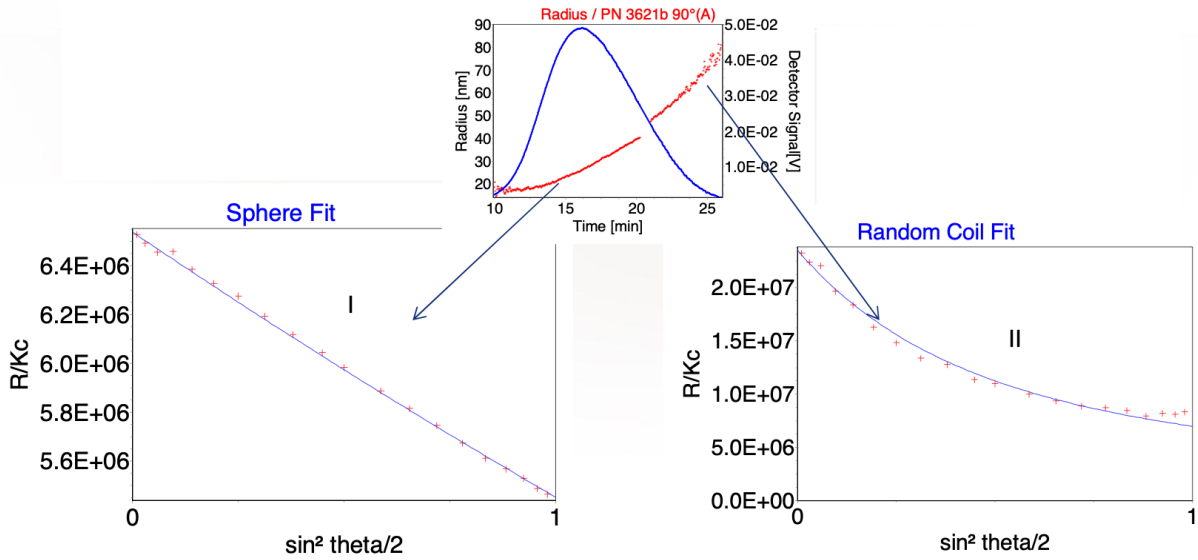

Figure S24: Data fitting of region I and II of T2.1 using a sphere fit and a random coil fit (see Figure 4, main manuscript).

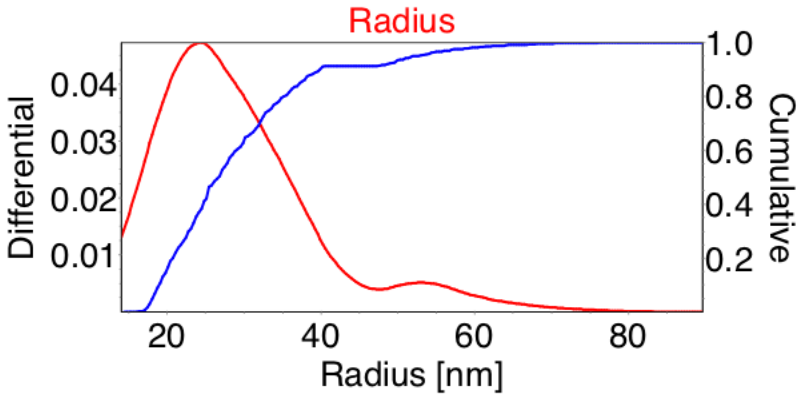

Figure S25: Differential Particle Size Distribution (red trace) and cumulative Particle Size Distribution (blue trace) of sample T2.1.

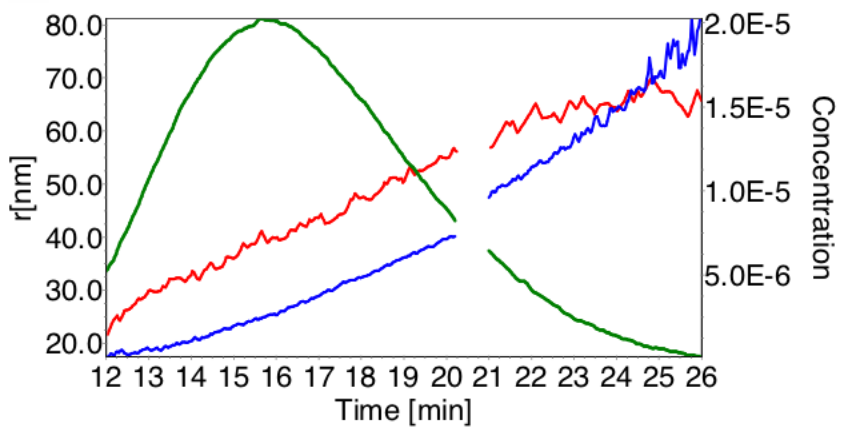

Figure S26: Overlay of the hydrodynamic radius (R_h from DLS; red), the radius of gyration (R_g from MALS; blue) and the concentration profile (green) of sample T2.1.

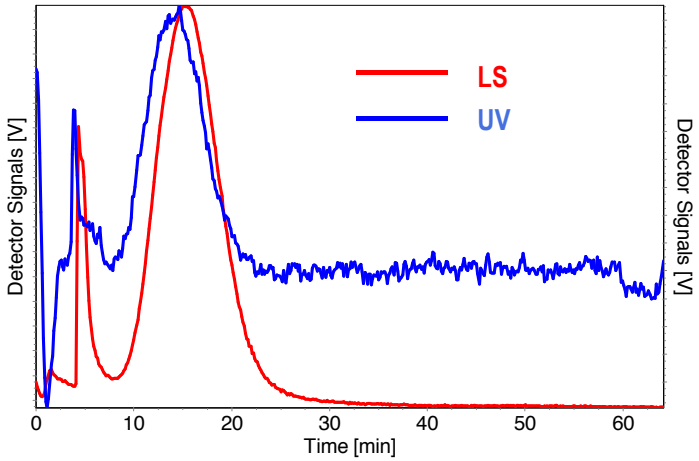

Figure S27: Raw Data Fractogram of AF4 – MALS & UV sample T2.2. The fractogram shows a system peak at ~7 min.

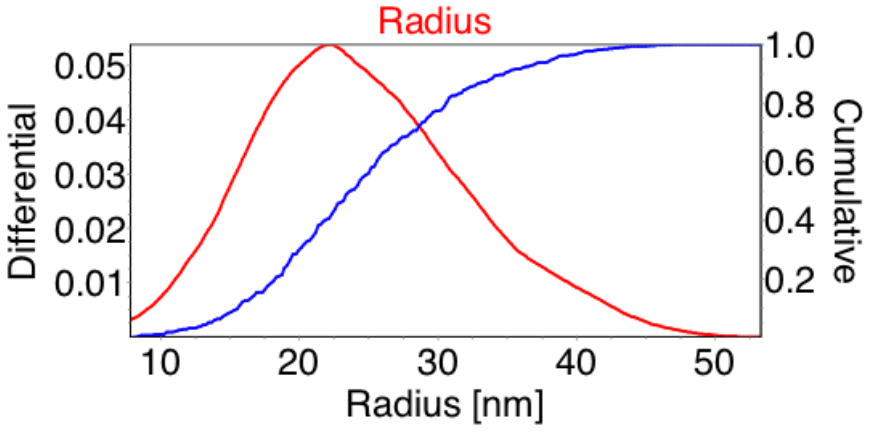

Figure S28: Differential Particle Size Distribution (red trace) and cumulative Particle Size Distribution (blue trace) of sample T2.2.

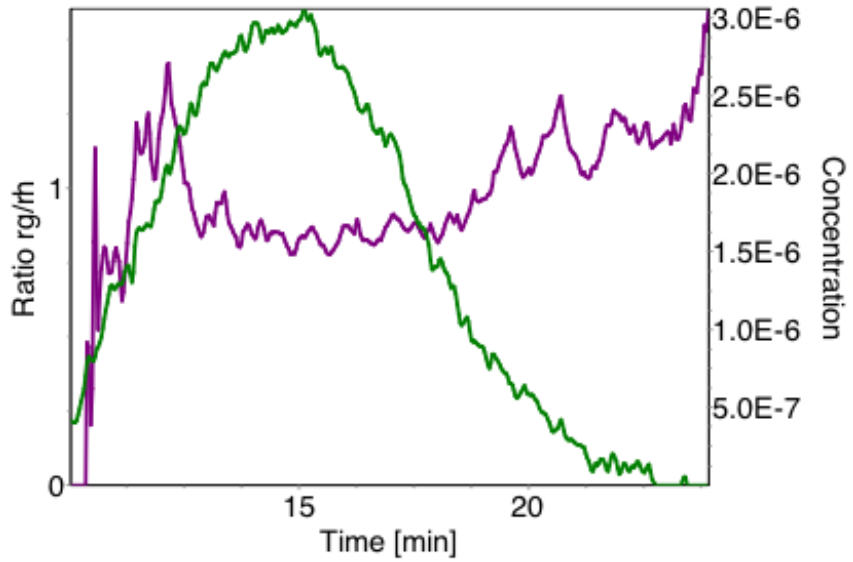

Figure S29: Overlay of the ratio of the R_g to R_h (purple) and the concentration profile (green) against elution time of sample T2.2.

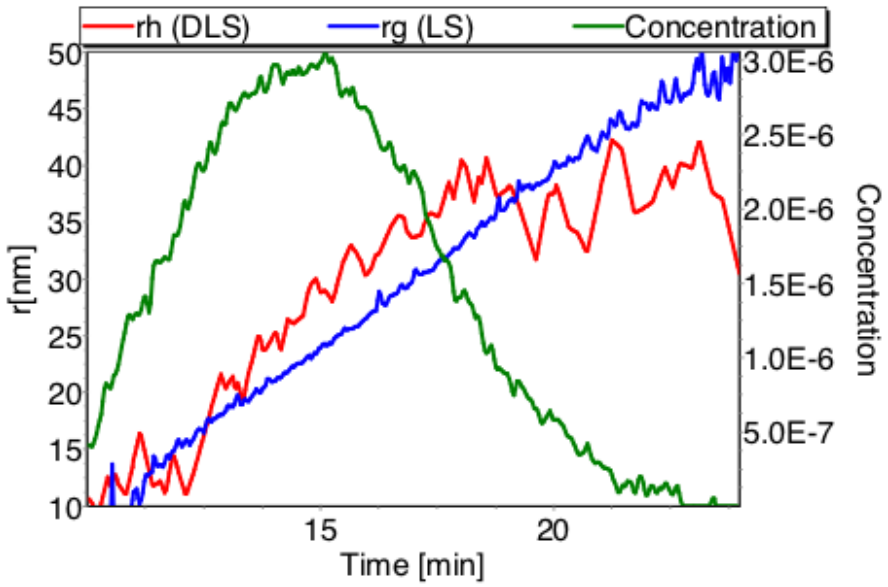

Figure S30: Overlay of the hydrodynamic radius (R_h from DLS; red), the radius of gyration (R_g from MALS; blue) and the concentration profile (green) of sample T2.2.

6. DLS experiments

6.1 DLS from THF solvent exchange procedure

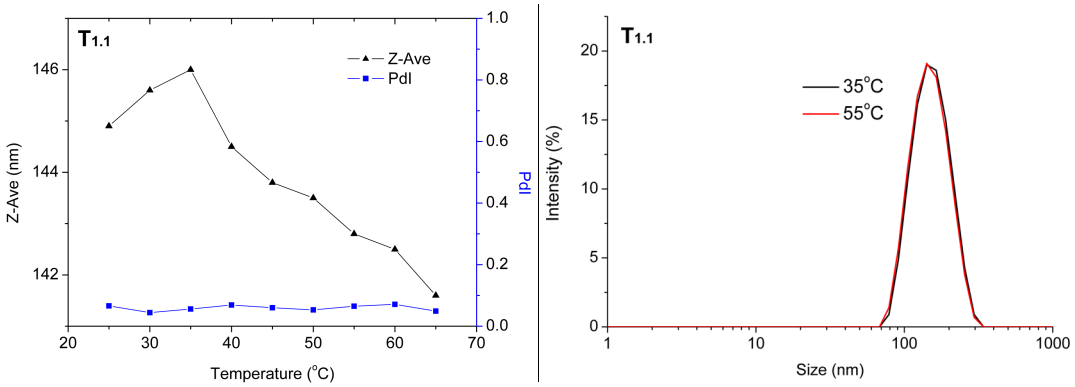

Figure S31: DLS traces of $T_{1.1}$ particles solutions obtained from THF.

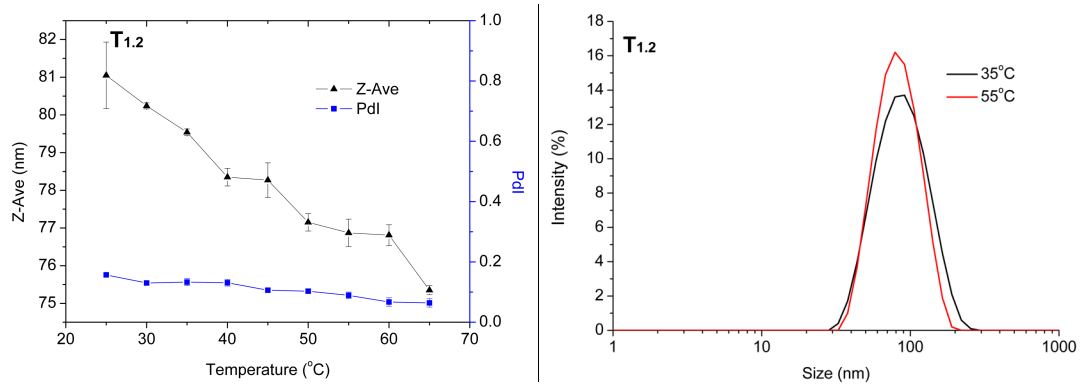

Figure S32: DLS traces of $T_{1.2}$ particles solutions obtained from THF.

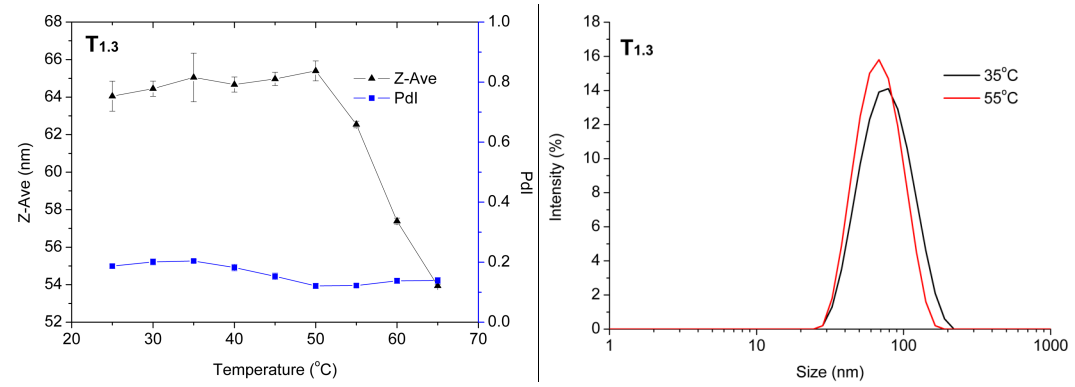

Figure S33: DLS traces of $T_{1.3}$ particles solutions obtained from THF.

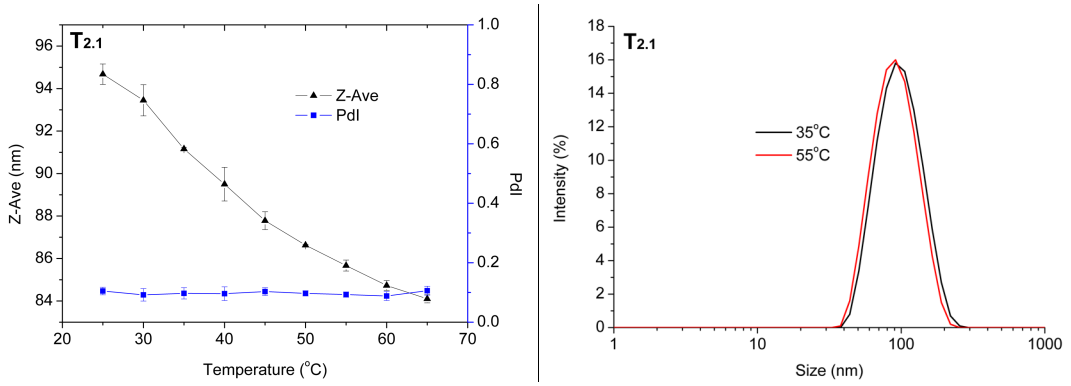

Figure S34: DLS traces of T $_{2.1}$ particles solutions obtained from THF.

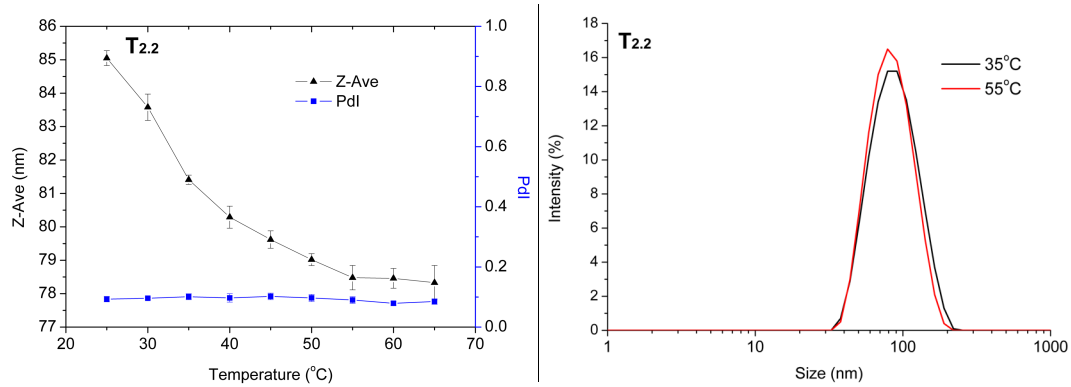

Figure S35: DLS traces of T $_{2.2}$ particles solutions obtained from THF.

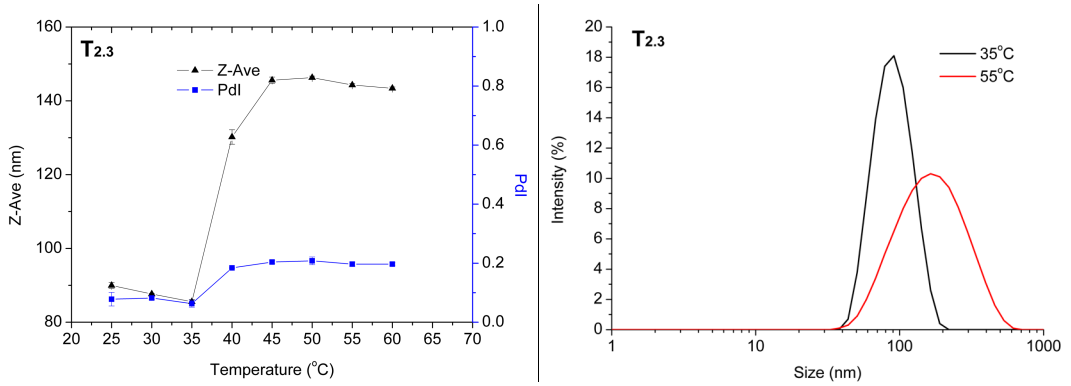

Figure S36: DLS traces of T $_{2.3}$ particles solutions obtained from THF.

6.2 DLS from HFIP solvent exchange procedure

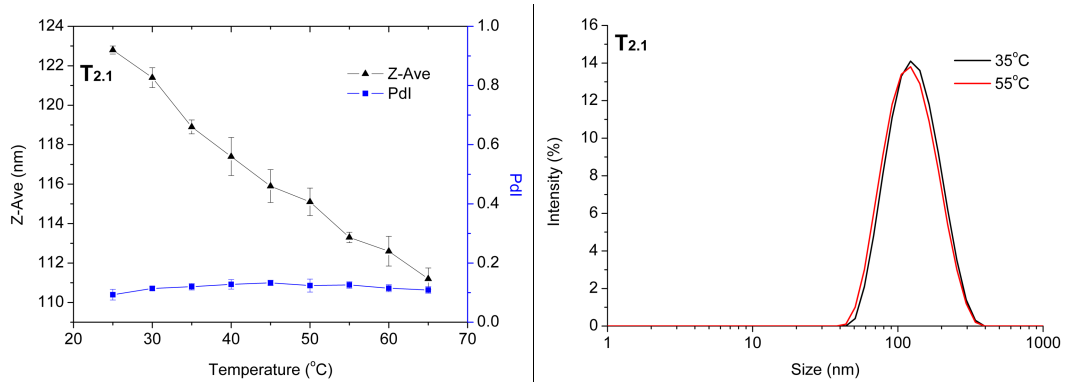

Figure S37: DLS traces of T $_{2.1}$ particles solutions obtained from HFIP.

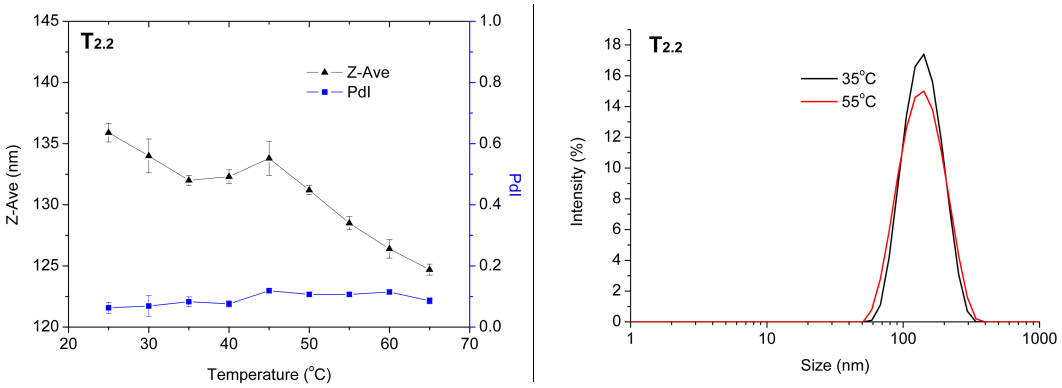

Figure S38: DLS traces of T $_{2.2}$ particles solutions obtained from HFIP.